Microbiome-based correction for random errors in nutrient profiles derived from self-reported dietary assessments

Tong Wang[1], Yuanqing Fu[2,3,4], Menglei Shuai[2,3,5], Ju-Sheng Zheng[2,3,4], Lu Zhu[6], Andrew T. Chan[1,4,7,8,9], Qi Sun[1,10,11], Frank B. Hu[1,10,11], Scott T. Weiss[1], Yang-Yu Liu[1,12,*]

[1]*Channing Division of Network Medicine, Department of Medicine, Brigham and Women's Hospital, Harvard Medical School, Boston, MA 02115, USA*

[2]*School of Life Sciences, Westlake University, Hangzhou, China*

[3]*Westlake Laboratory of Life Sciences and Biomedicine, Hangzhou, China*

[4]*Institute of Basic Medical Sciences, Westlake Institute for Advanced Study, Hangzhou, China*

[5]*Broad Institute of MIT and Harvard, Cambridge, MA 02142, USA*

[6]*Department of Epidemiology, University of Iowa College of Public Health, Iowa City, IA 52242, USA*

[7]*Clinical and Translational Epidemiology Unit, Massachusetts General Hospital and Harvard Medical School, Boston, MA 02114, USA*

[8]*Division of Gastroenterology, Massachusetts General Hospital and Harvard Medical School, Boston, MA 02114, USA*

[9]*Department of Immunology and Infectious Diseases, Harvard T.H. Chan School of Public Health, Boston, MA 02115, USA*

[10]*Department of Nutrition, Harvard T.H. Chan School of Public Health, Boston, MA 02115, USA*

[11]*Department of Epidemiology, Harvard T.H. Chan School of Public Health, Boston, MA 02115, USA*

[12]*Center for Artificial Intelligence and Modeling, The Carl R. Woese Institute for Genomic Biology, University of Illinois at Urbana-Champaign, Urbana, IL 61801, USA*

* Correspondence: yyl@channing.harvard.edu

Abstract

Since dietary intake is challenging to directly measure in large-scale cohort studies, we often rely on self-reported instruments (e.g., food frequency questionnaires, 24-hour recalls, and diet records) developed in nutritional epidemiology. Those self-reported instruments are prone to measurement errors, which can lead to inaccuracies in the calculation of nutrient profiles. Currently, few computational methods exist to address this problem. In the present study, we introduce a deep-learning approach --- **M**icrobiom**e**-based nu**t**rient p**r**ofi**l**e **c**orrector (METRIC), which leverages gut microbial compositions to correct random errors in self-reported dietary assessments using 24-hour recalls or diet records. We demonstrate the excellent performance of METRIC in minimizing the simulated random errors, particularly for nutrients metabolized by gut bacteria in both synthetic and three real-world datasets. Further research is warranted to examine the utility of METRIC to correct actual measurement errors in self-reported dietary assessment instruments.

Introduction

An unhealthy diet can increase the risk of many diseases[1,2,3,4]. For instance, excess intake of sugar or saturated fat could elevate the risk of coronary heart disease[5–8]. The investigation of the association between poor dietary habits and chronic diseases requires an accurate assessment of dietary intake in large population samples. Typically, epidemiologic studies rely on self-reported instruments such as food frequency questionnaires (FFQ)[9], Automated Self-Administered 24-hour Dietary Assessment Tool (ASA24)[10], and 7-Day Dietary Record (7DDR)[11], to collect diet data in large populations. However, self-reported instruments are subject to both random and systematic measurement errors[12–15]. While random errors are largely due to day-to-day individual variations in dietary intakes, systematic errors can be caused by under- or over-reporting and inaccurate estimation of portion sizes[16]. Measurement errors in the assessed food intake will be naturally propagated forward to the computation of the nutrient profile, causing inaccuracies in the assessed nutrient profile (Fig. 1a). Correcting such errors in the nutrient profile is crucial for improving the quality of nutritional epidemiology research. Several methods, such as regression calibrations[17,18] and cumulative averages[19] using repeated dietary assessments, have been used to correct for random errors of habitual diets in nutritional studies. These methods involve using a regression model to map the habitual dietary intake measured by a less accurate method (such as FFQ) to a more accurate habitual dietary measurement method (such as the average of 7DDRs). However, it is important to note that these methods are designed specifically to address measurement errors in habitual dietary intake and are incapable of correcting random measurement errors in single-day dietary assessments.

Signal reconstruction from corrupted or incomplete measurements is a common problem in various fields of research. For example, image denoising (i.e., removing noise from a noisy image to restore the true image) is an important topic in computer vision. The recent advance in deep neural networks has led to new methods that learn to map corrupted images to unobserved clean ones[20,21]. However, training those methods typically requires clean images, which are difficult to obtain in many cases. To overcome this challenge, a new class of methods that only leverages noisy images in training has been developed[22,23]. One noticeable example is Noise2Noise[22], which restores clean images by only being trained on corrupted ones. When the noise is random with a mean of zero, its performance is comparable and sometimes even better than other methods

trained using clean images[22]. The Noise2Noise's underlying principle involves training the model on pairs of noisy images as both input and output. This strategy forces the neural network to predict the average of the corrupted images, thereby statistically converging the prediction of Noise2Noise towards the clean image due to the zero-mean nature of the noise[22].

Inspired by the success of Noise2Noise[22], we hypothesize that we can correct the random error in the assessed nutrient profile derived from the self-reported dietary assessment without using clean data (i.e., the ground truth dietary intake). Note that we focus on correcting the nutrient profile instead of the food profile (or the original dietary assessment) because the prevalence of zero values in the food profile (i.e., no consumption for many food items) renders a big challenge for machine learning tasks, while the derived nutrient profile usually has non-zero values. Also, we focus on the correction for random errors with zero means instead of systematic bias/errors with non-zero means because effectively correcting the latter requires the ground truth dietary intake, which is typically not available.

Our key idea is to incorporate gut microbial compositions as part of the input of a deep-learning model and to infer the true nutrient profile based on the assessed nutrient profile and the measured gut microbial composition (Fig. 1b). This idea is based on the knowledge that many dietary constituents reaching the large intestine fuel the growth of gut microbes[24–26]. One example is the growth of gut microbes enabled by anaerobic fermentation of indigestible polysaccharides[24,25]. As a result, the gut microbial composition is linked to dietary intake. Advances in sequencing technologies have made it possible to determine the gut microbial composition quickly and accurately. It has been shown that fecal bacteria and metabolites can be used as biomarkers for predicting whether a few food items are introduced as dietary interventions (e.g., avocado) for healthy adults in dietary intervention studies[27,28]. Hence, using objective microbial biomarkers to infer dietary intake might complement the self-reported dietary assessment and thus reduce measurement error in dietary intake. In this work, we developed a deep-learning method: **M**icrobiom**e**-based nu**t**rient p**r**ofi**i**le **c**orrector (METRIC). We demonstrated the effectiveness of METRIC in removing randomly added noise to both synthetic and real data.

Results

Overview of METRIC

We aim to infer the true nutrient profile based on the assessed one and the measured gut microbial composition. A naive way to do this is to train a machine-learning model with the assessed nutrient profiles and microbial compositions as the input and the true nutrient profiles as the output. However, this is not feasible because such training requires the true nutrient profiles that are not easily available. To address this issue, we developed METRIC that does not rely on the true nutrient profile during its training but still can remove random errors in the assessed nutrient profile during testing (Fig. 2). During the training, we generated the corrupted nutrient profiles by adding random noise to the assessed nutrient profiles, and then trained METRIC to remove the added noise by taking the corrupted nutrient profiles and the measured microbial compositions as its input and generating the assessed nutrient profiles as its output (Fig. 2a). We introduced the corrupted nutrient profiles to avoid METRIC copying the assessed nutrient profiles directly to the output, thus forcing METRIC to remove the added noise. Note that the training of METRIC did not use true nutrient profiles.

The architecture of METRIC is a neural network that consists of three hidden layers, in addition to its input and output layers (Fig. 2b). Each hidden layer has a fixed dimension of 256. The link weights in the neural network are initialized using the Xavier Initialization. The training loss is the mean squared error. The predictive performance is assessed by the mean Pearson correlation coefficient between true and predicted nutrient concentrations averaged across all nutrients $\bar{\rho}$. One unique feature is the skip connection that adds the corrupted nutrient profiles directly to the final output of neural networks, which previously has been shown to enhance the training and predictive performance for deep neural networks[29]. Similar to the existence of the skip connection in Noise2Noise[22], the introduction of the skip connection enables the neural networks to adjust the prediction based on the corrupted nutrient profile, ensuring that output variables would not deviate too much from the corrupted nutrient profile. More details about the architecture can be found in the Methods section. Overall, METRIC is a generic "denoiser" that learns to remove any random noise added to the nutrient profile. With this generic ability to remove random noise, the well-trained METRIC should be able to remove random measurement errors by generating predictions closer to the true nutrient

142 profiles when it takes the assessed nutrient profiles and microbial compositions as its
143 input (Fig. 2c).
144 We split each dataset into two non-overlapping parts: a training and a test set.
145 METRIC was trained on the training set and then used to generate predictions for the test
146 set. The correction performance is measured by comparing the predicted nutrient profiles
147 with the "true" nutrient profiles in the test set (how we obtain the "true" nutrient profiles for
148 each scenario will be explained in separate sections below). To measure the predictive
149 performance of each nutrient, we adopted the Pearson Correlation Coefficient ρ between
150 its predicted and true corrected values.
151

152 ## METRIC can reduce measurement errors in nutrient profiles of synthetic data

153 We first validated METRIC using synthetic data for which we know the ground truth. We
154 used the Microbial Consumer-Resource Model (MiCRM)[30] to generate three types of data:
155 (1) *true* nutrient profiles (i.e., the ground-truth nutrient consumption), (2) *assessed*
156 nutrient profiles (i.e., the true nutrient profiles with random noise added to mimic
157 measurement errors), and (3) *corrupted* nutrient profiles (i.e., the assessed nutrient
158 profiles with artificially added random noise). MiCRM simulates the process of nutrient
159 consumption by microbes and the following microbial growth[30]. Note that the random
160 noise added to assessed and corrupted nutrient profiles are different. For simplicity, we
161 only considered the nutrient consumption in MiCRM and did not model the nutrient
162 production because most dietary nutrients cannot be produced by microbes. We created
163 different samples by randomly sampling nutrient fluxes and then running the community
164 assembly until we achieved a steady state. We consider sampled ground-truth nutrient
165 fluxes as true nutrient profiles and the steady-state microbial abundances as microbial
166 compositions. Gaussian noise $\mathrm{N}(0, \sigma^2)$ with the mean of zero and standard deviation σ
167 is added to true nutrient profiles to create assessed nutrient profiles. More details about
168 MiCRM, the generation of synthetic data, and added noise can be found in the Methods
169 section.
170 We generated 250 samples by simulating the assembly process for 250
171 independent communities with 20 nutrients and 20 bacterial species. We trained METRIC
172 on 200 samples and tested it on the remaining 50 samples. We measured how assessed
173 values and corrected values (i.e., predicted values on the test set) respectively correlate
174 with true values. For each nutrient, we measured ρ between its corrected values from

175 predictions and its true concentration (denoted as ρ_c). Similarly, we calculated ρ between
176 its assessed concentrations and its true concentration (denoted as ρ_a). As the standard
177 deviation σ of the Gaussian noise increases, METRIC starts to correct the introduced
178 noise, represented by the switch from negative values of $(\rho_c - \rho_a)$ to positive values in
179 Fig. 3a. It is natural to expect that the correction of nutrient profiles with weaker noises
180 does not work ($\rho_c < \rho_a$ for small σ in Fig. 3a), because the correction is not necessary
181 when the measurement error is small (e.g., when $\rho_a > 0.8$). We focus on the case of $\sigma =$
182 1.5 from now on. The difference between the two metrics (i.e., $\rho_c - \rho_a$) reflects the
183 correction performance. The nutrient in Fig. 3d-e is slightly corrected ($\rho_c - \rho_a = 0.01$),
184 while the nutrient in Fig. 3f-g is strongly corrected ($\rho_c - \rho_a = 0.09$). Most nutrients have a
185 better alignment between their corrected values and true values (Fig. 3h).
186

187 ## METRIC mitigates measurement errors added to nutrient profiles in real data

188 Next, we tested METRIC on three real-world datasets. The first dataset, MCTS
189 (MiCrobiome dieT Study), comes from a unique study that investigated the influence of
190 diets on gut microbial composition[31]. It is unique because a large number of samples
191 (n=210) of paired nutrient profiles and microbial compositions were collected. The nutrient
192 profiles were calculated from ASA24 (see Methods). Different from the availability of true
193 nutrient profiles in synthetic data, the true nutrient profiles are not available for real data.
194 To deal with this issue, we treated the nutrient profiles derived from ASA24 as the "true"
195 nutrient profiles and added random noise (Gaussian noise with the mean of zero and
196 standard deviations σ) to them as "assessed" nutrient profiles. As σ increases, METRIC
197 starts to better correct the introduced noise (Fig. 4a). We focus on the case of $\sigma = 1.0$
198 from now on. We found that carotene has a large ρ_a and is not improved by METRIC
199 ($\rho_a = 0.99$ versus $\rho_c = 0.97$ in Figs. 4b-c). By contrast, fiber has a small ρ_a and is strongly
200 improved ($\rho_a = 0.35$ versus $\rho_c = 0.58$ for Figs. 4f-g). We believe that the large correction
201 in the total fiber intake was due to most fibers being digested by gut microbes[24,25]. Overall,
202 nutrients with smaller ρ_a have better correction performance, and nutrients with large ρ_a
203 rarely improved (Fig. 4h). The mean correction performance averaged over all nutrients
204 is $(\overline{\rho_c} - \overline{\rho_a}) = 0.079$.
205 We also tried to run METRIC without using the microbial composition, finding that
206 the correction performance ($\overline{\rho_c} - \overline{\rho_a} = 0.067$) is worse than that with included microbial
207 composition (Supplementary Fig. 1). We also computed the sensitivity which is defined

as the ratio between the reduction in ρ of nutrient α and the perturbation amount of species i (Supplementary Fig. 2), which could detect some possible interactions between nutrients and species. For example, the sensitivity of monounsaturated fatty acids towards *Bacteroides uniformis* is large (~0.025, larger than 99.98% of the inferred sensitivity values), and is supported by the previously observed reduction of monounsaturated fatty acids by *Bacteroides uniformis*[32]. In addition, our sensitivity analysis revealed that the top three microbial taxa linked to fiber content correction, which exhibit the highest sensitivity values, are well-documented as fiber degraders in the literature: *Bacteroides plebeius*[33], *Parabacteroides sp*[34], and *Bacteroides sp*[35].

Then, we applied METRIC to the second dataset MLVS (Men's Lifestyle Validation Study)[36,37]. Specifically, we utilized the composition of gut microbiomes and the one-day dietary assessment of the 7-day dietary records (7DDRs). The 7DDRs are widely recognized to be the most reliable estimation of dietary intake because participants are required to measure and report gram weights for foods both before they start eating and after they finish, thereby enabling the calculation of the actual food consumption based on the difference in weight[38]. To guarantee the usefulness of gut microbial composition in correcting dietary assessment, we required the identification of paired microbial compositions and dietary assessments with matching dates. In MLVS, a total of 599 paired samples with matching dates were found. Similarly, as we did for the MCTS dataset, we regarded the nutrient profile derived from the 7DDRs as the "true" nutrient profile and added varying levels of Gaussian noise to it as the "assessed" nutrient profile. Then we trained METRIC on 80% of the data and tested it on the remaining 20%. Consistent with our previous findings, the trained METRIC exhibits an ability to correct the nutrient profile (Fig. 5a), especially for large σ. For the case of $\sigma = 1.0$, the mean correction performance ($\overline{\rho_c} - \overline{\rho_a}$) is 0.072 (Fig. 5h). Across all nutrients, dietary fiber was the strongest corrected nutrient (Figs. 5f-g).

Finally, we applied METRIC to the third dataset WE-MACNUTR (Westlake N-of-1 Trials for Macronutrient Intake)[39]. WE-MACNUTR is a dietary intervention study that implemented a 'complete feeding' strategy, providing three isocaloric meals per day to 28 participants over a span of 72 days. Each participant completed high-fat, low-carbohydrate and low-fat, high-carbohydrate diets in a randomized sequence, with a 6-day wash-out period between them. Since the diets were completely controlled and well-documented, the nutrient profile derived from this dataset closely reflects the true nutrient profile. In WE-MACNUTR, we found 317 paired samples with both microbial compositions

and nutrient profiles. Considering the nutrient profile from the complete feeding as the true nutrient profile, we introduced varying levels of noise (Gaussian noise $\mathrm{N}(0, \sigma^2)$ with different standard deviations σ) to create the assessed nutrient profile. Like our earlier results, METRIC can correct the nutrient profile when σ is large (Fig. 6a). When $\sigma = 1.0$, the mean correction performance $(\overline{\rho_c} - \overline{\rho_a})$ is 0.118 (Fig. 6h) and dietary fiber again exhibits a substantial correction (Figs. 6f-g).

To provide a more representative picture of METRIC's robustness and effectiveness across different noise levels, we also investigated situations where the correction is less effective for all three datasets (standard deviation of the noise $\sigma = 0.5$; Supplementary Figs. 3-5). Although the overall correction performance $(\bar{\rho}_c - \bar{\rho}_a)$ is weak when $\sigma = 0.5$, the correction still works well for nutrients with smaller ρ_a (e.g., dietary fibers). We also evaluated the predictive performance using a more quantitative metric, the mean absolute error. We found that the overall pattern in correction performance measured by mean absolute error aligns with that measured by Pearson correlation across datasets (Supplementary Figs. 6-8). For the MLVS and WE-MACNUTR datasets, we also tried to evaluate METRIC's correction performance without using the microbial composition, finding that the correction performance is comparable to that achieved when the microbial composition is included (Supplementary Figs. 9&10). This implies that METRIC can still be leveraged to correct nutrient profiles even in the absence of gut microbial compositions.

We capitalized on the longitudinal nature of the MCTS dataset to explore whether increasing temporal offsets between microbiome and diet data impacts the correction efficiency of our method. Specifically, we increased the offset by aligning the diet of day t with the microbiome of day $t + \Delta t$ and subsequently correcting nutrient profiles. Our analysis reveals that the correction performance progressively decreases as the offset Δt deviates from 1 day (Supplementary Fig. 11). This serves as a validation of METRIC, as it indicates that microbiome-diet relationships are causal.

Given the absence of ground-truth nutrient profiles for direct validation, we instead conducted an indirect validation of our method by checking if the noise level of real-life nutrient profiles is within the regime where we can remove the random measurement errors well. We found that the correction performance of METRIC is great when the mean Pearson correlation coefficient $\bar{\rho}_a$ is below 0.8 (Figs. 4-6). Due to the lack of ground-truth nutrient profiles to directly quantify the noise level, we can only approximate this indirectly by reflecting the nutrient variability using the multiple-day 7DDRs in MLVS. Specifically,

we calculated the Pearson correlation coefficient ρ between concentrations of a nutrient derived from one 7DDR and its average values obtained from multiple 7DDRs for seven consecutive days (Supplementary Fig. 12a). We found that the mean Pearson correlation coefficient $\bar{\rho}$ is 0.77, which is below 0.8. Additionally, 62.0% of 329 nutrients have $\rho < 0.8$. A similar analysis on the dataset MCTS revealed that $\bar{\rho} = 0.63$ and 95.0% of nutrients have $\rho < 0.8$ (Supplementary Fig. 12b). The WE-MACNUTR dataset was not analyzed due to the absence of dietary assessments. These findings across both datasets confirm that the approximated noise levels are within a range where METRIC is effective at correcting random measurement errors.

We also examined the impact of noise with a non-zero mean by introducing the Gaussian noise $\mathrm{N}(\mu, \sigma^2)$. For the three datasets we used, we set $\sigma = 1$ as this is the regime where our method, METRIC, consistently shows strong correction performance. We then gradually increased the mean of the noise μ from 0.0 to 2.0 to create the assessed nutrient profile. When applying METRIC to remove the noise, we observed that its correction performance diminishes to zero as μ increases (Supplementary Figs. 13-15), indicating that METRIC can remove the random error but not the systematic drift or shift.

Discussion

We presented a deep-learning method, METRIC, to correct random simulated measurement errors in the nutrient profile. The method relies on the assessed nutrient profile and microbial composition to learn how to infer the true nutrient profile. First, we validated its performance on synthetic data where we directly modeled true and assessed nutrient profiles. Then we applied METRIC to three distinct real clinical datasets with added noise to the nutrient profile and found that it can correct the nutrient profile well, especially for nutrients with large errors or metabolized by gut microbes. Similar to the class of computational methods that denoise images even without clean targets[22,23], METRIC offers a significant advantage by being capable of correcting the random measurement error without using the true nutrient profiles during the training. This attribute makes our method particularly useful in real-life scenarios where only assessed nutrient profiles are available, without access to true nutrient profiles.

We admit that METRIC has several limitations. First, without using clean targets (i.e., the ground truth dietary intake), METRIC is only capable of removing random

measurement errors that have zero means. It cannot remove noise with a non-zero mean, just like Noise2Noise[22]. Thus, METRIC cannot correct the systematic bias/drift/error (with a non-zero mean) in nutrient profiles. Effectively correcting the systematic bias requires both assessed and true nutrient profiles to discern the consistent deviation between them. However, it is very unlikely that both assessed and true nutrient profiles are available to measure the real systematic bias in real-world data. If both types of nutrient profiles are available, it remains to be investigated whether it is possible to design a regression model that predicts true nutrient profiles based on assessed nutrient profiles, thereby achieving the task of removing the systematic bias. Second, METRIC uses microbial compositions of fecal samples to correct nutrient profiles derived from ASA24 or 7DDR, which were collected exactly one day prior to fecal sample collection. We do not expect that microbial compositions of fecal samples collected from a particular time point could be used to correct nutrient profiles derived from FFQ, where subjects report how often each food item was consumed over a specified period, typically the past month or year. To clearly demonstrate this point, we leveraged the FFQ, 7DDR, and gut microbiome data from MLVS to compare the performance of using gut microbial compositions to predict the 7DDR- or FFQ-based nutrient profiles. We found that the predictability of FFQ-based nutrient profiles is much worse than that of 7DDR-based nutrient profiles (Supplementary Fig. 16). Consequently, we believe that METRIC cannot be used to correct random errors in FFQ-based nutrient profiles.

We recognize the challenges of applying a model trained on one dataset to another, particularly when biases like sequencing errors or differences in nutrient databases are present. However, training the method on one dataset and generating predictions for the other is possible if both datasets were collected and processed in the same way. For example, in the PRISM and NLIBD studies, two Inflammatory Bowel Disease cohorts—one from Boston (n=155) and an external validation cohort from the Netherlands (n=65)—were collected using the same protocols. This standardization enables accurate predictions of disease status in the NLIBD cohort by a machine learning method trained on the PRISM data[40]. Similarly, the deep-learning model mNODE trained on PRISM data showed great performance in predicting fecal metabolome based on gut microbial compositions from the NLIBD cohort[41].

There are other methods to improve the accuracy of dietary intake measurement over traditional self-reported dietary assessments. For instance, digital documentation of meals through taking photos can be used to improve the accuracy of dietary assessment,

though the validity of such technologies is yet to be established. In addition, nutritional biomarkers such as DNA barcodes for plants[42] and metabolite biomarkers[28,43,44] have been utilized to improve the assessment of food intake. A more accurate reflection of nutrient consumption can be obtained by using objective measurements of microbial composition or metabolomic profile, which can complement self-reported dietary assessment tools. Currently, an active research direction in the field of precision nutrition is to identify microbial and metabolite biomarkers for dietary intake. Although several studies attempted to predict the presence of food items based on fecal bacteria and metabolites[27,28], the analyses were limited to several food items and no connection to nutrient profiles was examined. Further research is warranted to examine the utility of METRIC to correct actual measurement errors in self-reported dietary assessments.

Methods

Datasets. The first dataset we used comes from a study that investigated the association between diet and the gut microbiome[31]. The study has paired 24-h food records and fecal shotgun metagenomes from 34 healthy human subjects collected daily over 17 days, with 210 paired samples in total. The second dataset is from MLVS[36,37] with 599 paired gut microbial compositions and 7DDRs. The third dataset is from WE-MACNUTR[39], a dietary intervention study that provides three meals per day for all participants. The study involved 30 participants, with 2 participants withdrawing from the trial early and not included in the final analysis. It has 317 paired gut microbial compositions and true nutrient profiles of complete feeding with matching dates. For all machine learning tasks, the same five random 80/20 train-test splits were utilized to guarantee a fair comparison of methods.

The generation of nutrient profiles based on dietary assessments. The generation of nutrient profiles generated from dietary assessments involves several steps and relies on comprehensive food composition databases such as USDA's Food and Nutrient Database for Dietary Studies (FNDDS)[45] or Harvard Food Composition Database (HFDB)[46], etc. Each food item consumed is matched with a corresponding item in a food composition database. These databases provide detailed information on the nutrient content of food items, including macronutrients (e.g., fats, proteins, carbohydrates) and micronutrients (e.g., vitamins and minerals). By multiplying the amount of each food

consumed by its nutrient content, the total intake of each nutrient is calculated to obtain the nutrient profiles. For example, the MCTS dataset utilized ASA24 to collect dietary intake data, where documented foods were assigned to nutrients based on the USDA's FNDDS 2011-2012[45]. In the case of the MLVS dataset, nutrient intake was derived from 7DDRs using the Nutrition Data System for Research[47], which provides a comprehensive food and nutrient database managed by the University of Minnesota Nutrition Coordinating Center. For the WE-MACNUTR dataset, which focuses on a Chinese population, nutrient profiles were derived from the foods directly provided to participants using the electronic version of China Food Composition Tables (Standard Edition)[48].

The generation of synthetic data. Similar to the traditional consumer-resource model[49,50] and Microbial Consumer-Resource Model[30], we simulated the process of nutrient consumption by microbes and the following microbial growth. For simplicity, we assumed a global pool with 20 microbial species and 20 nutrients in total. To mimic the difference in nutrient consumption profiles across individuals, we randomly assigned flux for each sample: to create a unique sample, the supply rate of each nutrient is randomly drawn from a uniform distribution $\mathcal{U}[0,1]$. We recorded the assigned supply rates of all nutrients as the true nutrient profile. The Gaussian noise with a mean of 0 and standard deviation of 0.5 is added to true nutrient profile to create assessed nutrient profiles with measurement errors. After the assignment of nutrient fluxes, we simulated the community assembly dynamics until the system reaches a steady state. The steady-state microbial relative abundances are recorded as the microbial composition for the sample. Then we repeated this procedure of generating samples 250 times, forming the synthetic dataset we used in this study. The 250 samples are split in the 80/20 ratio as the training/test set.

The overall population dynamics for the concentration of nutrient N_α and abundance of microbial species M_i can be written as follows:

$$\frac{dN_\alpha}{dt} = -\sum_i a_{i\alpha} M_i N_\alpha - \delta N_\alpha,$$

$$\frac{dM_i}{dt} = \frac{\sum_\gamma a_{i\gamma} M_i N_\gamma}{Y} - \delta M_i,$$

where $a_{i\alpha}$ is the consumption rate of nutrient α by the species i, δ is the dilution rate, and Y is the yield. For simplicity, we assumed $\delta = 0.1$ and $Y = 1$. The $a_{i\alpha}$ is assumed to be non-zero with a probability of 50%. If $a_{i\alpha}$ is non-zero, its value is drawn from the uniform distribution $\mathcal{U}[0,10]$. Eventually, each $a_{i\alpha}$ is divided by the number of nutrients that can be consumed by the species i, avoiding the outgrowth of generalists.

METRIC. The core of METRIC is the MLP (Multilayer Perceptron).

- Data processing: The Centered Log-Ratio transformation is applied to microbial relative abundances, and the log transformation is applied to the nutrient profiles.
- Model detail: METRIC has 3 hidden layers in the middle, sandwiched by input and output variables. Each hidden layer has a fixed hidden layer dimension of 256. The Xavier Initialization is used to initialize the weights in the neural network. A skip connection from corrupted nutrient profiles is introduced to add to the final layer of MLP. Specifically, the final prediction is the sum of (1) the corrupted input from the skip connection multiplied by a weight parameter α and (2) the final layer of MLP multiplied by $(1-\alpha)$. The optimal value for α is chosen based on the five-fold cross-validation results on the training set.
- Training method: The Adam optimizer[51] is used for the gradient descent. The training loss is the mean squared error. The training stops when the mean Pearson Correlation Coefficient of nutrients $\bar{\rho}$ on the validation/test set starts to decrease within the past 10 epochs.
- Activation function: ReLU (Rectified Linear Unit).

Statistics. To calculate correlation throughout the study, we used Pearson's correlation coefficient. All simulations and analyses were performed using standard numerical and scientific computing libraries such as NumPy and SciPy in the Python programming language (version 3.7.1) and Jupyter Notebook (version 6.1).

Data availability. We only used the data collected by existing studies. Instructions for downloading sequencing data and dietary intakes analyzed in this work can be found in the literature exploring MCTS (MiCrobiome dieT Study)[31], MLVS (Men's Lifestyle Validation Study)[36,37], and WE-MACNUTR (Westlake N-of-1 Trials for Macronutrient Intake)[39]. To facilitate the data downloading, the URLs to those datasets are also provided in our GitHub repository (https://github.com/wt1005203/METRIC).

Code availability. All code for simulations used in this manuscript can be found at https://github.com/wt1005203/METRIC.

Acknowledgements. We acknowledge grants from the National Institutes of Health (R01AI141529, R01HD093761, R35CA253185, RF1AG067744, UH3OD023268, U19AI095219, U01HL089856, U01-152905, and U01-167552) and Cancer Grand

Challenges Team PROSPECT. We thank Walter Willett, Eric Rimm, and Lorelei Mucci for valuable discussions.

Author contributions. T.W. and Y.-Y.L. designed the project. T.W. performed all the numerical calculations and data analysis. T.W. processed the real data with assistance from Y.Fu. All authors analyzed the results. T.W. and Y.-Y.L. wrote the paper. All authors edited and approved the paper.

Correspondence. Correspondence and requests for materials should be addressed to Y.-Y. L. (email: yyl@channing.harvard.edu).

Competing Interests. The authors declare no competing interests.

References

1. Afshin, A. *et al.* Health effects of dietary risks in 195 countries, 1990–2017: a systematic analysis for the Global Burden of Disease Study 2017. *The Lancet* **393**, 1958–1972 (2019).
2. Mozaffarian, D. *et al.* Global Sodium Consumption and Death from Cardiovascular Causes. *New England Journal of Medicine* **371**, 624–634 (2014).
3. Hu, F. B. Diet strategies for promoting healthy aging and longevity: An epidemiological perspective. *Journal of Internal Medicine* **n/a**,.
4. Donaldson, M. S. Nutrition and cancer: A review of the evidence for an anti-cancer diet. *Nutrition Journal* **3**, 19 (2004).
5. Hu, F. B. & Willett, W. C. Optimal Diets for Prevention of Coronary Heart Disease. *JAMA* **288**, 2569–2578 (2002).
6. Mensink, R. P., Zock, P. L., Kester, A. D. & Katan, M. B. Effects of dietary fatty acids and carbohydrates on the ratio of serum total to HDL cholesterol and on serum lipids and apolipoproteins: a meta-analysis of 60 controlled trials. *The American Journal of Clinical Nutrition* **77**, 1146–1155 (2003).
7. DiNicolantonio, J. J., Lucan, S. C. & O'Keefe, J. H. The Evidence for Saturated Fat and for Sugar Related to Coronary Heart Disease. *Progress in Cardiovascular Diseases* **58**, 464–472 (2016).
8. Malik, V. S. & Hu, F. B. The role of sugar-sweetened beverages in the global epidemics of obesity and chronic diseases. *Nat Rev Endocrinol* **18**, 205–218 (2022).
9. McNutt, S., Zimmerman, T. P. & Hull, S. G. Development of food composition databases for food frequency questionnaires (FFQ). *Journal of Food Composition and Analysis* **21**, S20–S26 (2008).
10. Sharpe, I. *et al.* Automated Self-Administered 24-H Dietary Assessment Tool (ASA24) recalls for parent proxy-reporting of children's intake (> 4 years of age): a feasibility study. *Pilot and Feasibility Studies* **7**, 123 (2021).
11. Hebert, J. R. *et al.* Development and testing of a seven-day dietary recall. *Journal of Clinical Epidemiology* **50**, 925–937 (1997).
12. Westerterp, K. R. & Goris, A. H. C. Validity of the assessment of dietary intake: problems of misreporting. *Current Opinion in Clinical Nutrition & Metabolic Care* **5**, 489 (2002).
13. Poslusna, K., Ruprich, J., Vries, J. H. M. de, Jakubikova, M. & Veer, P. van't. Misreporting of energy and micronutrient intake estimated by food records and 24 hour recalls, control and adjustment methods in practice. *British Journal of Nutrition* **101**, S73–S85 (2009).
14. Dao, M. C. *et al.* Dietary assessment toolkits: an overview. *Public Health Nutrition* **22**, 404–418 (2019).
15. Ravelli, M. N. & Schoeller, D. A. Traditional Self-Reported Dietary Instruments Are Prone to Inaccuracies and New Approaches Are Needed. *Frontiers in Nutrition* **7**, (2020).
16. Willett, W. Correction for the Effects of Measurement Error. in *Nutritional Epidemiology* (ed. Willett, W.) 0 (Oxford University Press, 2012). doi:10.1093/acprof:oso/9780199754038.003.0012.
17. Rosner, B., Willett, W. C. & Spiegelman, D. Correction of logistic regression relative risk estimates and confidence intervals for systematic within-person measurement error. *Statistics in Medicine* **8**, 1051–1069 (1989).
18. Spiegelman, D., McDermott, A. & Rosner, B. Regression calibration method for correcting measurement-error bias in nutritional epidemiology. *The American Journal of Clinical Nutrition* **65**, 1179S-1186S (1997).

19. Hu, F. B. *et al.* Dietary Fat and Coronary Heart Disease: A Comparison of Approaches for Adjusting for Total Energy Intake and Modeling Repeated Dietary Measurements. *American Journal of Epidemiology* **149**, 531–540 (1999).
20. Schmidt, U. & Roth, S. Shrinkage Fields for Effective Image Restoration. in 2774–2781 (2014).
21. Chen, Y. & Pock, T. Trainable Nonlinear Reaction Diffusion: A Flexible Framework for Fast and Effective Image Restoration. *IEEE Transactions on Pattern Analysis and Machine Intelligence* **39**, 1256–1272 (2017).
22. Lehtinen, J. *et al.* Noise2Noise: Learning Image Restoration without Clean Data. in *Proceedings of the 35th International Conference on Machine Learning* 2965–2974 (PMLR, 2018).
23. Krull, A., Buchholz, T.-O. & Jug, F. Noise2Void - Learning Denoising From Single Noisy Images. in 2129–2137 (2019).
24. Donia, M. S. & Fischbach, M. A. Small molecules from the human microbiota. *Science* **349**, 1254766 (2015).
25. Koh, A., De Vadder, F., Kovatcheva-Datchary, P. & Bäckhed, F. From Dietary Fiber to Host Physiology: Short-Chain Fatty Acids as Key Bacterial Metabolites. *Cell* **165**, 1332–1345 (2016).
26. Santhiravel, S. *et al.* The Impact of Plant Phytochemicals on the Gut Microbiota of Humans for a Balanced Life. *International Journal of Molecular Sciences* **23**, 8124 (2022).
27. Shinn, L. M. *et al.* Fecal Bacteria as Biomarkers for Predicting Food Intake in Healthy Adults. *The Journal of Nutrition* **151**, 423–433 (2021).
28. Shinn, L. M. *et al.* Fecal Metabolites as Biomarkers for Predicting Food Intake by Healthy Adults. *The Journal of Nutrition* nxac195 (2022) doi:10.1093/jn/nxac195.
29. He, K., Zhang, X., Ren, S. & Sun, J. Deep Residual Learning for Image Recognition. in *2016 IEEE Conference on Computer Vision and Pattern Recognition (CVPR)* 770–778 (IEEE, Las Vegas, NV, USA, 2016). doi:10.1109/CVPR.2016.90.
30. Marsland, R. *et al.* Available energy fluxes drive a transition in the diversity, stability, and functional structure of microbial communities. *PLoS Comput Biol* **15**, e1006793 (2019).
31. Johnson, A. J. *et al.* Daily Sampling Reveals Personalized Diet-Microbiome Associations in Humans. *Cell Host & Microbe* **25**, 789-802.e5 (2019).
32. López-Almela, I. *et al.* Bacteroides uniformis combined with fiber amplifies metabolic and immune benefits in obese mice. *Gut Microbes* **13**, 1–20 (2021).
33. Um, C. Y. *et al.* Grain, Gluten, and Dietary Fiber Intake Influence Gut Microbial Diversity: Data from the Food and Microbiome Longitudinal Investigation. *Cancer Research Communications* **3**, 43–53 (2023).
34. Wei, W. *et al.* Parabacteroides distasonis uses dietary inulin to suppress NASH via its metabolite pentadecanoic acid. *Nat Microbiol* **8**, 1534–1548 (2023).
35. Yang, J. *et al.* High Soluble Fiber Promotes Colorectal Tumorigenesis Through Modulating Gut Microbiota and Metabolites in Mice. *Gastroenterology* **166**, 323-337.e7 (2024).
36. Mehta, R. S. *et al.* Stability of the human faecal microbiome in a cohort of adult men. *Nat Microbiol* **3**, 347–355 (2018).
37. Li, J. *et al.* Interplay between diet and gut microbiome, and circulating concentrations of trimethylamine N-oxide: findings from a longitudinal cohort of US men. *Gut* **71**, 724–733 (2022).
38. Yue, Y. *et al.* Reproducibility and validity of diet quality scores derived from food-frequency questionnaires. *The American Journal of Clinical Nutrition* **115**, 843–853 (2022).

555 39. Ma, Y. *et al.* Individual Postprandial Glycemic Responses to Diet in n-of-1 Trials:
556 Westlake N-of-1 Trials for Macronutrient Intake (WE-MACNUTR). *The Journal of*
557 *Nutrition* **151**, 3158–3167 (2021).
558 40. Franzosa, E. A. *et al.* Gut microbiome structure and metabolic activity in
559 inflammatory bowel disease. *Nat Microbiol* **4**, 293–305 (2019).
560 41. Wang, T. *et al.* Predicting metabolomic profiles from microbial composition
561 through neural ordinary differential equations. *Nat Mach Intell* **5**, 284–293 (2023).
562 42. Reese, A. T. *et al.* Using DNA Metabarcoding To Evaluate the Plant Component
563 of Human Diets: a Proof of Concept. *mSystems* **4**, e00458-19 (2019).
564 43. Guasch-Ferré, M., Bhupathiraju, S. N. & Hu, F. B. Use of Metabolomics in
565 Improving Assessment of Dietary Intake. *Clinical Chemistry* **64**, 82–98 (2018).
566 44. Brennan, L., Hu, F. B. & Sun, Q. Metabolomics Meets Nutritional Epidemiology:
567 Harnessing the Potential in Metabolomics Data. *Metabolites* **11**, 709 (2021).
568 45. FNDDS : USDA ARS. https://www.ars.usda.gov/northeast-area/beltsville-md-
569 bhnrc/beltsville-human-nutrition-research-center/food-surveys-research-
570 group/docs/fndds/#.
571 46. Colditz, G. A., Manson, J. E. & Hankinson, S. E. The Nurses' Health Study: 20-
572 Year Contribution to the Understanding of Health Among Women. *Journal of Women's*
573 *Health* **6**, 49–62 (1997).
574 47. Feskanich, D., Sielaff, B. H., Chong, K. & Buzzard, I. M. Computerized collection
575 and analysis of dietary intake information. *Computer Methods and Programs in*
576 *Biomedicine* **30**, 47–57 (1989).
577 48. Yang, Y. & Wang, Z. China food composition tables standard edition. *Peking*
578 *University Medical Press: Beijing, China* (2018).
579 49. MacArthur, R. Species packing and competitive equilibrium for many species.
580 *Theoretical Population Biology* **1**, 1–11 (1970).
581 50. Chesson, P. MacArthur's consumer-resource model. *Theoretical Population*
582 *Biology* **37**, 26–38 (1990).
583 51. Kingma, D. P. & Ba, J. Adam: A Method for Stochastic Optimization. Preprint at
584 https://doi.org/10.48550/arXiv.1412.6980 (2017).
585
586

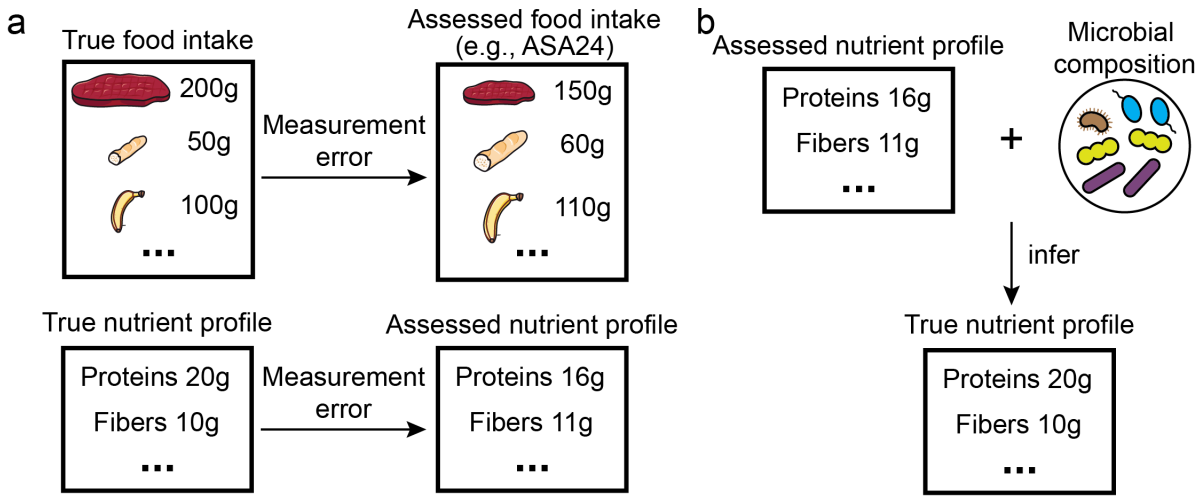

Figure 1: **The idea of inferring the true nutrient profile based on the assessed nutrient profile and microbial composition. a,** The typical dietary assessment such as ASA24 (Automated Self-Administered 24-hour Dietary Assessment Tool) often induces a measurement error in the food intake due to unreliable mental recall. Such a random measurement error or systematic error/bias in the food intake is carried to the nutrient profile when the food profile is converted to the nutrient profile. **b,** Our goal in this study is to remove the random part of measurement error. More specifically, we would like to infer true nutrient profiles based on assessed nutrient profiles and microbial compositions.

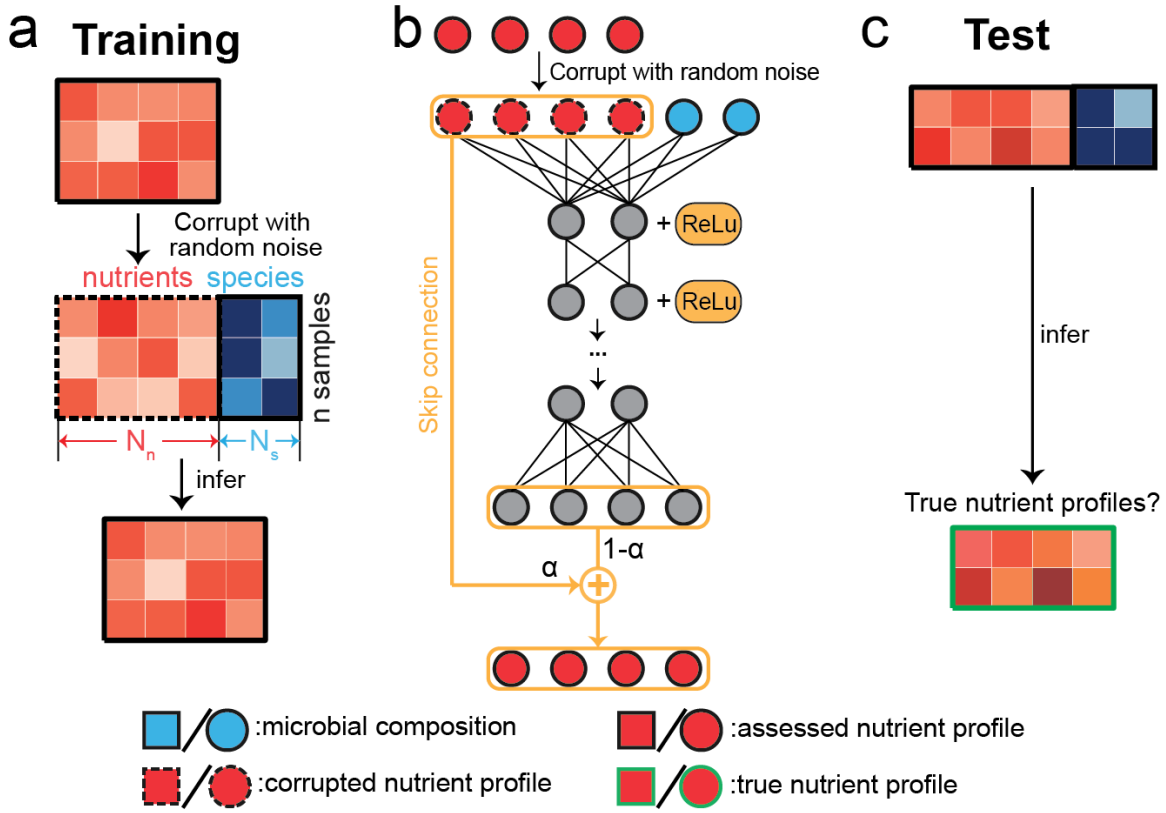

Figure 2: **The architecture and workflow of METRIC to infer true nutrient profiles.** For simplicity, we used a hypothetical example with n=3 training samples and 2 samples in the test set. For each sample, there are N_s microbial species and N_n nutrients. Across panels, microbial species and their relative abundances are colored blue. Nutrients and their amounts are colored red. The corrupted nutrient profiles are created by adding different types of random noise (i.e., Gaussian, Uniform, etc.) to the assessed nutrient profiles. Icons associated with assessed/corrupted nutrient profiles are bounded by solid black/dashed lines. Icons associated with true nutrient profiles are bounded by solid green lines. **a,** During the training of METRIC, the method takes corrupted nutrient profiles and microbial compositions as the input and learns to infer assessed nutrient profiles. **b,** Similar to multilayer perceptrons, METRIC has several hidden layers in the middle. The skip connection provides the corrupted nutrient profile directly to one layer before the final output, enabling it to skip the propagation through the hidden layers. The skipped corrupted nutrient profile multiplied by the weight parameter α and the final hidden layer (the bottom grey nodes) multiplied by $(1-\alpha)$ add up as the final output (the bottom red nodes). **c,** The well-trained METRIC is applied to the test set to generate predictions for nutrient profiles whose values are compared to true nutrient profiles.

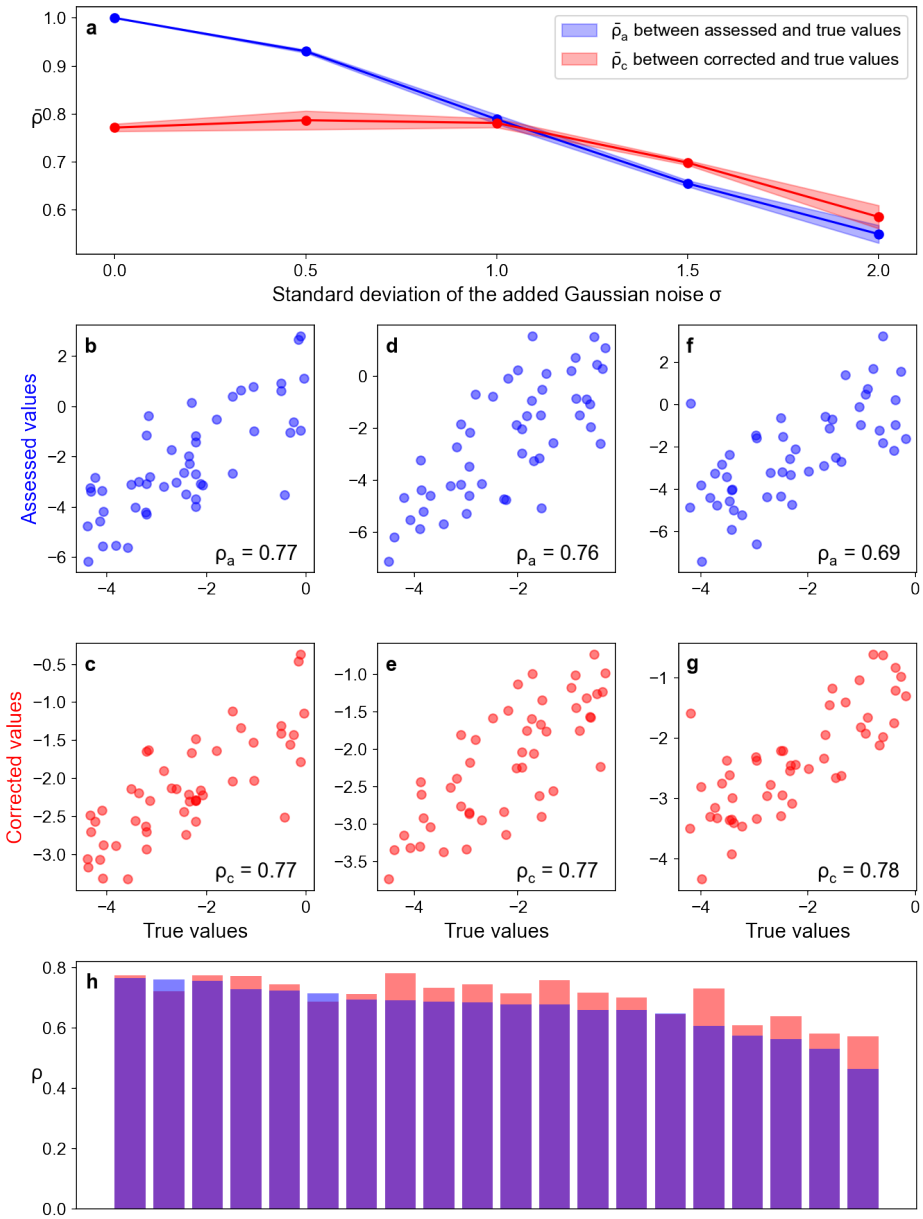

Figure 3: **METRIC can correct the measurement error in assessed nutrient profiles on synthetic data from MiCRM[30].** The Pearson's Rank Correlation Coefficient ρ is adopted to evaluate the correlation across various types of nutrient profiles. All corrected/true values shown are the log of nutrient concentrations. **a,** ρ_c (i.e., ρ between corrected and true values) and ρ_a (i.e., ρ between assessed and true values) decrease as the standard deviation of added Gaussian noise σ increases. All following panels focus on the case of σ=1.5. **b,** The correlation between assessed values and true values of log concentrations of one nutrient among different samples. **c,** The correlation between corrected values (predictions of METRIC) and true values of log concentrations of the same nutrient among different samples. Similar comparisons for another two nutrients are shown in **d-e** and **f-g**. **e,** The correction performance of all nutrients is measured by $(\rho_c - \rho_a)$.

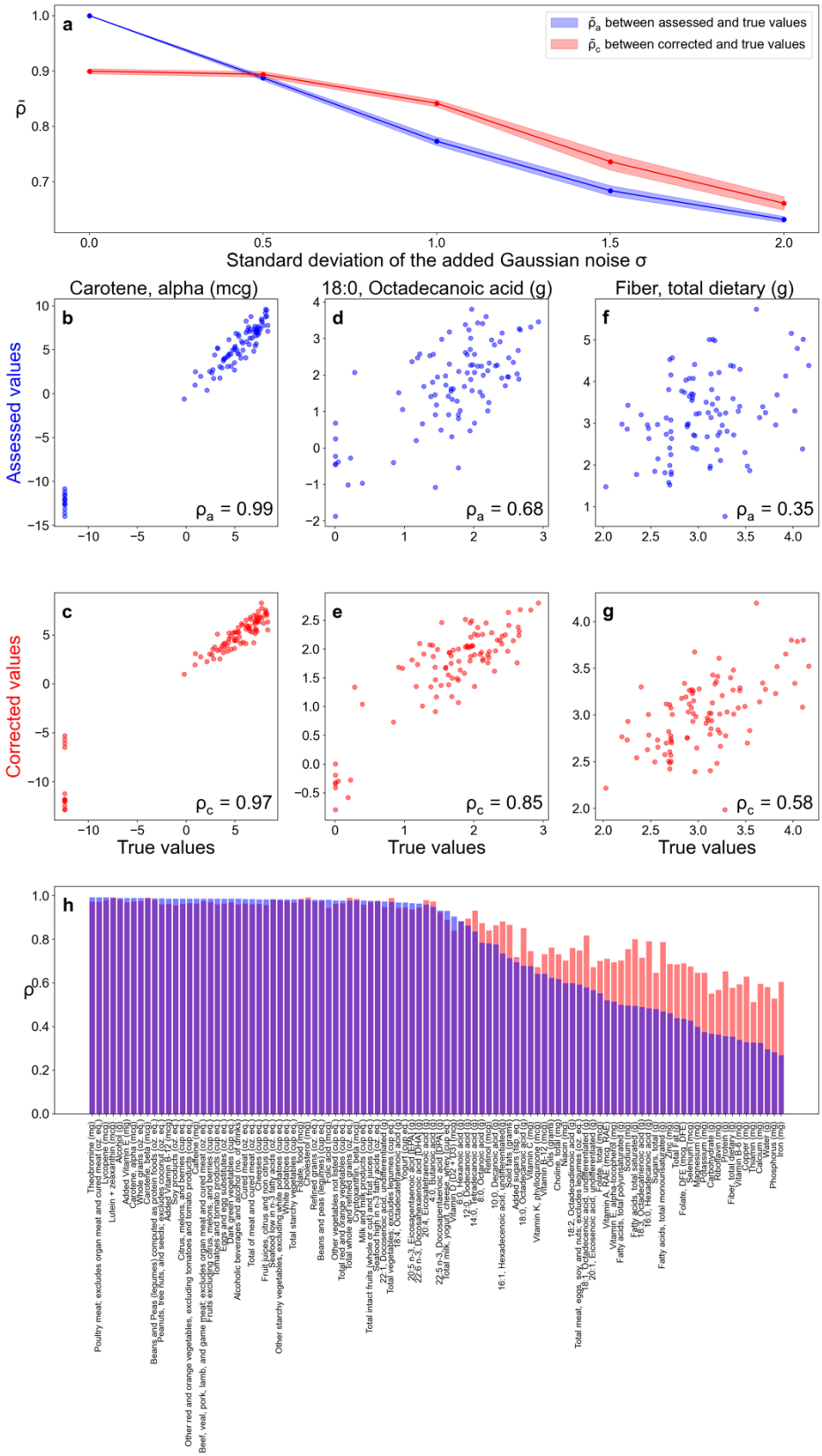

Figure 4: **METRIC can correct the measurement error in assessed nutrient profiles on real data from MCTS[31].** The Pearson's Rank Correlation Coefficient ρ is adopted to evaluate the correlation across various types of nutrient profiles. All nutrient concentrations are in the unit of grams. All corrected/true values shown are the log of nutrient concentrations. **a,** ρ_c (i.e., ρ between corrected and true values) and ρ_a (i.e., ρ between assessed and true values) decrease as the standard deviation of added Gaussian noise σ increases. All following panels focus on the case of σ=1.0. **b,** The correlation between assessed values and true values of log concentrations of carotene among different samples. **c,** The correlation between corrected values (predictions of METRIC) and true values of log concentrations of carotene among different samples. **d-e,** The similar comparison for octadecanoic acid shows a modest correction. **f-g,** The similar comparison for fiber shows a strong correction. **h,** The correction performance for all nutrients is measured by $(\rho_c - \rho_a)$.

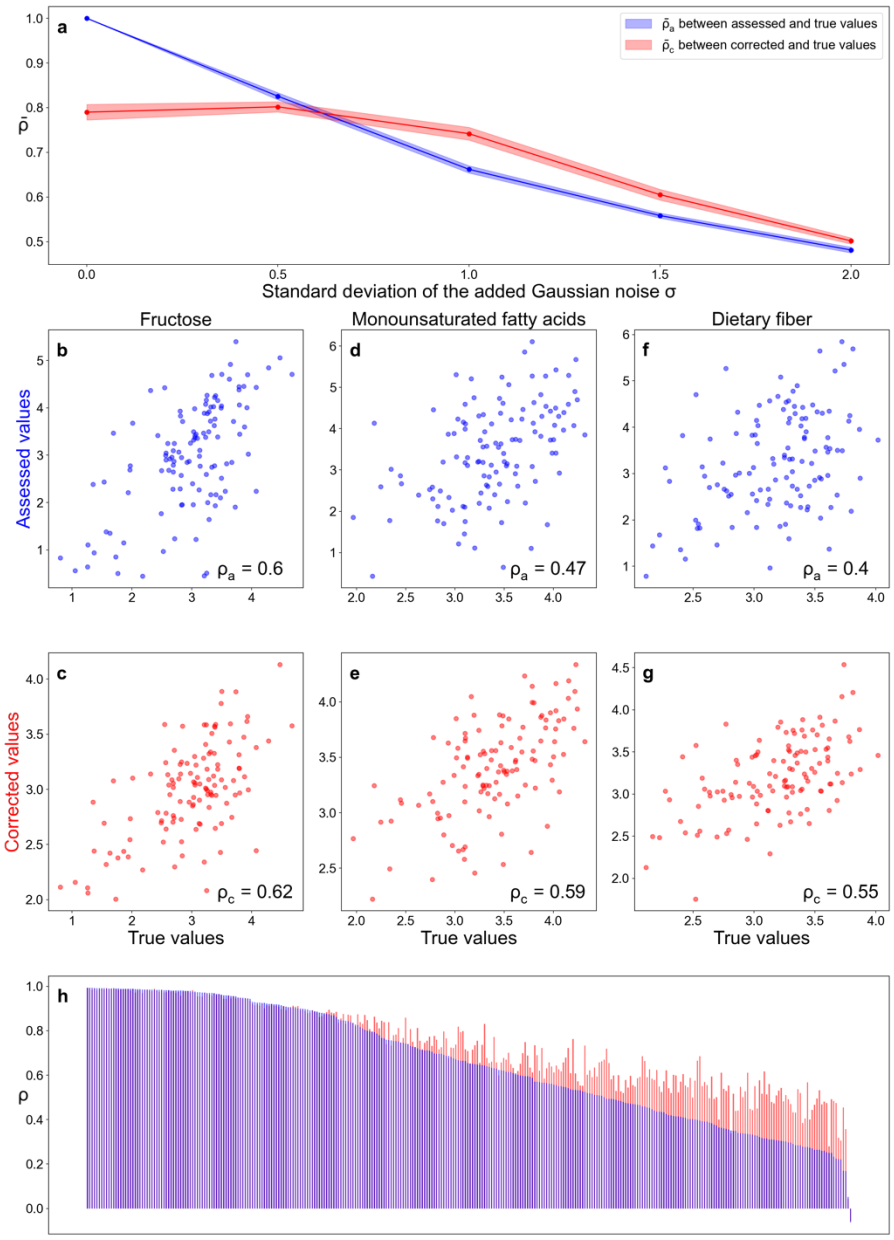

Figure 5: **METRIC can correct the measurement error in assessed nutrient profiles from MLVS**[36,37]**.** The Pearson's Rank Correlation Coefficient ρ is adopted to evaluate the correlation across various types of nutrient profiles. All nutrient concentrations are in the unit of grams. All corrected/true values shown are the log of nutrient concentrations. **a,** ρ_c (i.e., ρ between corrected and true values) and ρ_a (i.e., ρ between assessed and true values) decrease as the standard deviation of added Gaussian noise σ increases. All following panels focus on the case of σ=1.0. **b,** The correlation between assessed values and true values of log concentrations of fructose among different samples. **c,** The correlation between corrected values (predictions of METRIC) and true values of log concentrations of fructose among different samples. **d-e,** The similar comparison for monounsaturated fatty acids shows a modest correction. **f-g,** The similar comparison for dietary fiber shows a strong correction. **h,** The correction performance for all nutrients is measured by $(\rho_c - \rho_a)$. Nutrient names are not added due to lack of space.

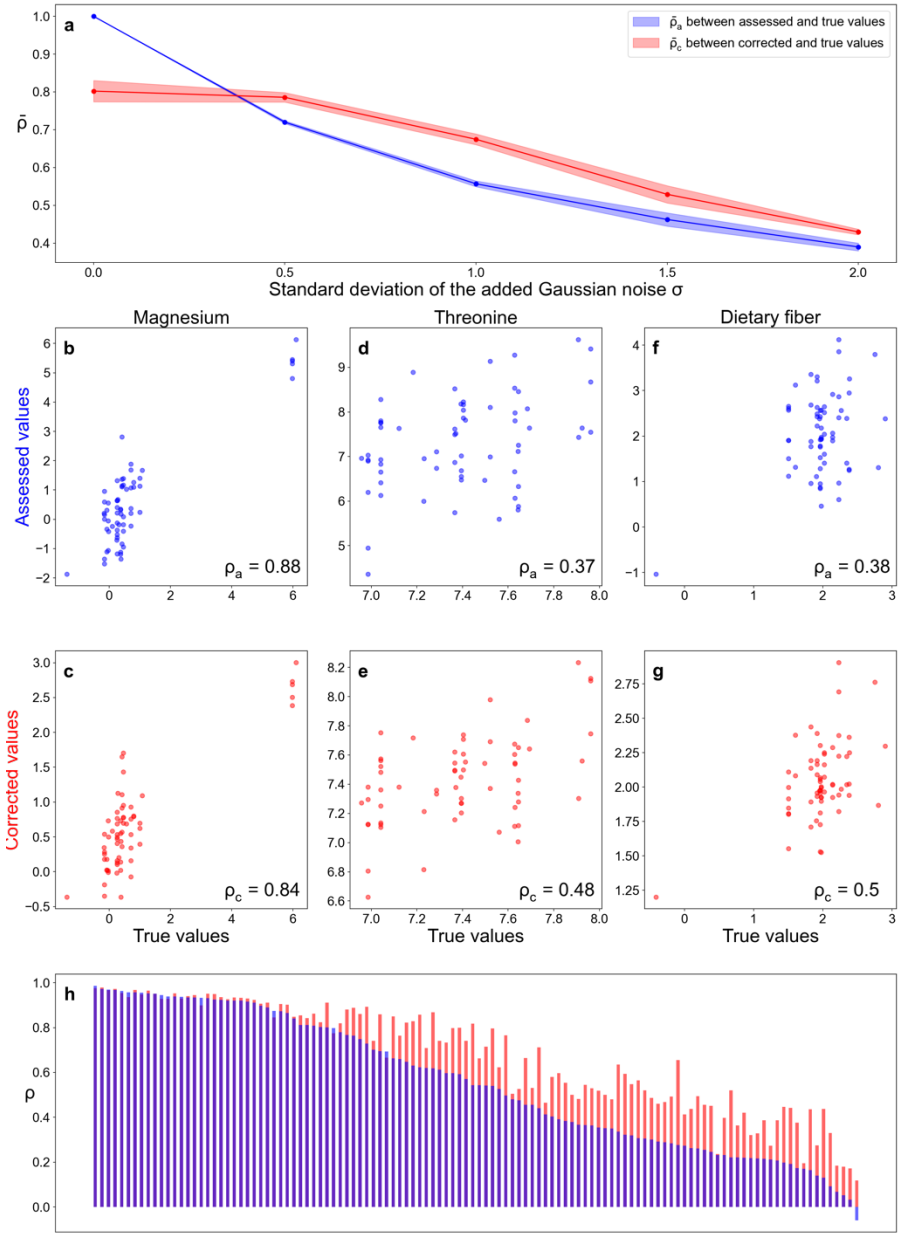

Figure 6: **METRIC can correct the measurement error in assessed nutrient profiles from WE-MACNUTR[39].** The Pearson's Rank Correlation Coefficient ρ is adopted to evaluate the correlation across various types of nutrient profiles. **a,** ρ_c (i.e., ρ between corrected and true values) and ρ_a (i.e., ρ between assessed and true values) decrease as the standard deviation of added Gaussian noise σ increases. All nutrient concentrations are in the unit of grams. All corrected/true values shown are the log of nutrient concentrations. All following panels focus on the case of σ=1.0. **b,** The correlation between assessed values and true values of log concentrations of magnesium among different samples. **c,** The correlation between corrected values (predictions of METRIC) and true values of log concentrations of magnesium among different samples. **d-e,** The similar comparison for threonine shows a modest correction. **f-g,** The similar comparison

671 for dietary fiber shows a strong correction. **h,** The correction performance for all nutrients
672 is measured by ($\rho_c - \rho_a$). Nutrient names are not added due to lack of space.